HUMAN MOVEMENT (ISSN 1899-1955)
2026; 27(1): 146–160

Influence of carbon fibre plate geometry on lower limb kinematic asymmetry in well-trained endurance runners: a biomechanical investigation

original paper
DOI: https://doi.org/10.5114/hm/216976

JIACHAO CAI[1,2,3], DONG SUN[1,2], YUFEI FANG[1], CHENGYUAN ZHU[2], FENGPING LI[2], YANG SONG[2,4], XUANZHEN CEN[2], TIBOR J. GODA[3], ZIXIANG GAO[5], YAODONG GU[1,2,6]

[1] Research Academy of Medicine Combining Sports, Ningbo No. 2 Hospital, Ningbo, China
[2] Faculty of Sports Science, Ningbo University, Ningbo, China
[3] Doctoral School on Safety and Security Sciences, Óbuda University, Budapest, Hungary
[4] Department of Biomedical Engineering, Faculty of Engineering, The Hong Kong Polytechnic University, Hong Kong SAR, China
[5] Human Performance Laboratory, Faculty of Kinesiology, University of Calgary, Calgary, AB, Canada
[6] Research Institute of Sport Science, Hungarian University of Sport Science, Budapest, Hungary

ABSTRACT

Purpose. This study explored how variations in the curvature of carbon fibre plates embedded in running shoes affect gait symmetry of the lower limbs in well-trained long-distance runners.

Methods. Sixteen well-trained runners participated in biomechanical testing under two shoe conditions (flat vs. curved carbon plates) using a Vicon 3D motion capture system (Oxford Metrics Ltd., Oxford, UK) and force plates. Symmetry angle (SA) was calculated for joint angles, moments, and stiffness to assess bilateral symmetry. SPM_1d (One-dimensional Statistical Parametric Mapping) was used to compare time-series joint angle data between shoe types. Two-way ANOVA examined peak joint moments and stiffness across limbs and shoe conditions, while paired *t*-tests assessed SA differences in joint range of motion, peak moments, and stiffness.

Results. The results showed that curved carbon plate shoes demonstrated better symmetry in peak ankle eversion and external rotation moments, peak knee external rotation moments and abduction–adduction stiffness, and hip rotational stiffness, suggesting that improved load distribution may help reduce the injury risk typically associated with asymmetric joint loading. In contrast, flat carbon plate shoes exhibited superior symmetry in hip rotational angles and knee flexion-extension stiffness, indicating potential advantages in promoting lower limb coordination.

Conclusions. These findings preliminarily suggest that the geometry of carbon fibre plates significantly influences lower limb biomechanical symmetry and dynamic characteristics, potentially regulating overall gait coordination through kinetic chain interactions. This study offers biomechanical insights to optimise running shoe design and improve performance and injury prevention in long-distance running.

Key words: running, footwear, sports injuries, biomechanics, asymmetry

Introduction

The midsole plays a pivotal role in running shoe design. Recently, carbon-fibre plates have become integral to midsoles due to their high stiffness and elastic rebound, which enhance propulsion efficiency and running economy. This innovation has been widely embraced by elite athletes and recreational runners for improving marathon performance [1].

Most studies on carbon-fibre plate design have focused on longitudinal bending stiffness or thickness, with limited attention to the impact of plate shape [2]. In practice, carbon plates can be flat or upward-curved ('spoon-shaped') to conform to the foot arch, and such geometric differences may affect foot mechanics, joint kinematics, and neuromuscular control during running [3, 4]. While stiffness is well-studied, the biomechanical effects of shape remain largely unexplored.

Correspondence address: Yufei Fang, Research Academy of Medicine Combining Sports, Ningbo No. 2 Hospital, No. 41, Xibei Road, Haishu District Ningbo, Zhejiang, 315099, China, e-mail: fyf369@126.com; https://orcid.org/0009-0002-8499-5772

Received: July 02, 2025
Accepted for publication: January 14, 2026

Citation: Cai J, Sun D, Fang Y, Zhu C, Li F, Song Y, Cen X, Goda TJ, Gao Z, Gu Y. Influence of carbon fibre plate geometry on lower limb kinematic asymmetry in well-trained endurance runners: a biomechanical investigation. Hum Mov. 2026;27(1): 146–160; doi: https://doi.org/10.5114/hm/216976.

This study addresses that gap using high-resolution motion capture and symmetry analysis. Running is a popular sport, but carries a high injury risk due to factors such as joint mechanics, foot structure, footwear, and training variables. Lower limb symmetry is essential for efficient movement and postural stability, yet many studies analyse only the dominant limb, overlooking asymmetry's effects on performance and injury [5, 6]. Evidence links asymmetry with injuries like tibial stress fractures, which often result from uneven load distribution [7, 8]. Fatigue can exacerbate asymmetries, particularly in knee joint rotation and stiffness. Iliotibial band syndrome and Achilles tendinitis have also been associated with asymmetric hip and ankle movement patterns [9–11]. Moreover, asymmetry tends to increase with running speed, potentially impairing performance and elevating injury risk [12].

Recent studies suggest that shoe modifications can influence step frequency and propulsion mechanics, thereby affecting lower limb symmetry during running [13]. Moreover, recent studies have shown that changes in foot strike pattern and plantar pressure distribution between minimalist and traditional running shoes, as well as the interaction between footwear type and lower-limb dominance, can substantially modulate running gait and asymmetry in more ecologically valid conditions [14, 15]. However, any functional enhancement must align with natural locomotor demands to avoid introducing new injury risks [16]. Although midsole stiffness, shoe weight, and upper design have been examined, there remains a lack of biomechanical evidence on how variations in carbon-fibre plate shapes influence limb asymmetry. Thus, investigating the effects of plate geometry on symmetry and its implications for injury risk is both necessary and timely. Recent advances in sports biomechanics have emphasised that new methods and technologies should be developed with two main objectives in mind: enhancing performance and reducing injury risk [17].

This study examined how flat and curved carbon-fibre plate designs affect lower limb symmetry during running. By comparing symmetry patterns across key joint variables, we aimed to determine whether plate geometry influences asymmetry and to identify which design better optimises symmetry, thereby informing functional running shoe design. Accordingly, this study tested the hypothesis that a curved carbon-fibre plate configuration would yield more symmetrical lower-limb kinetics than a flat-plate configuration, owing to its smoother rollover profile and load-transfer characteristics.

Material and methods

Participants

Sixteen well-trained, healthy male marathon runners (age: 27.72 ± 2.30 years; height: 1.72 ± 0.04 m; weight: 67.05 ± 5.16 kg; BMI: 21.27 ± 2.06 kg/m²) were recruited. Inclusion criteria included: age 18–34, right-leg dominance, rearfoot-to-forefoot running style, EU size 41 shoes, no recent injuries or gait abnormalities, and a marathon best under 2 h 55 min with a weekly mileage of 100–160 km.

Experimental shoes

Two visually identical pairs of EU size 41 running shoes were used, with the primary design difference being the shape of the embedded carbon-fibre plate (flat vs. curved). In addition to plate geometry, key parameters differed slightly between models, including shoe mass (208 g vs. 212 g), forefoot stack height (34 mm vs. 31 mm), rocker axis position (73% vs. 70%), and rocker radius (8.1 cm vs. 9.5 cm, all respectively). Stiffness was high in both models. Rocker geometry (rocker radius and rocker axis position) was quantified from standardised side-view images of the shoes by using the Kinovea software (https://www.kinovea.org/) to digitise points along the forefoot rocker line and fit a circular arc, from which the rocker radius and rocker axis position were derived [18]. Figure 1 presents these specifications and fluoroscopic images of participants wearing each shoe. All participants completed randomised running trials in both conditions at a consistent time of day to control for circadian effects.

Experimental protocol

Participants first familiarised themselves with the lab, had their height and weight recorded, and completed a treadmill warm-up. During testing, they wore standardised attire. Kinematic and kinetic data were collected using an eight-camera Vicon system (200 Hz) and AMTI force platforms (1000 Hz), synchronised for temporal alignment. Running speed was monitored via an infrared timing system (Brower Timing). Thirty-eight reflective markers were placed on anatomical landmarks to capture full-body motion. After static calibration, participants ran at 18 km/h along a 10 m runway with embedded force plates [19]. A valid trial required full foot contact on both plates during left–right heel strikes within a single stride. Five valid trials per shoe condition were recorded. To ensure consistency, participants maintained natural running form and rested for 10 s between trials.

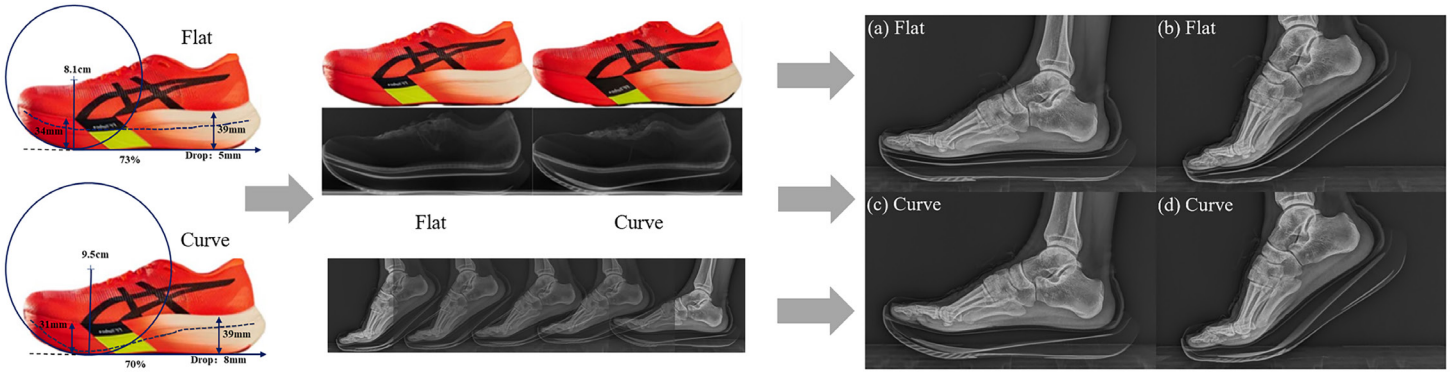

Figure 1. (a, b) show the foot posture during the mid-stance and toe-off phases while wearing flat carbon plate shoes, (c, d) show the corresponding phases while wearing curved carbon plate shoes

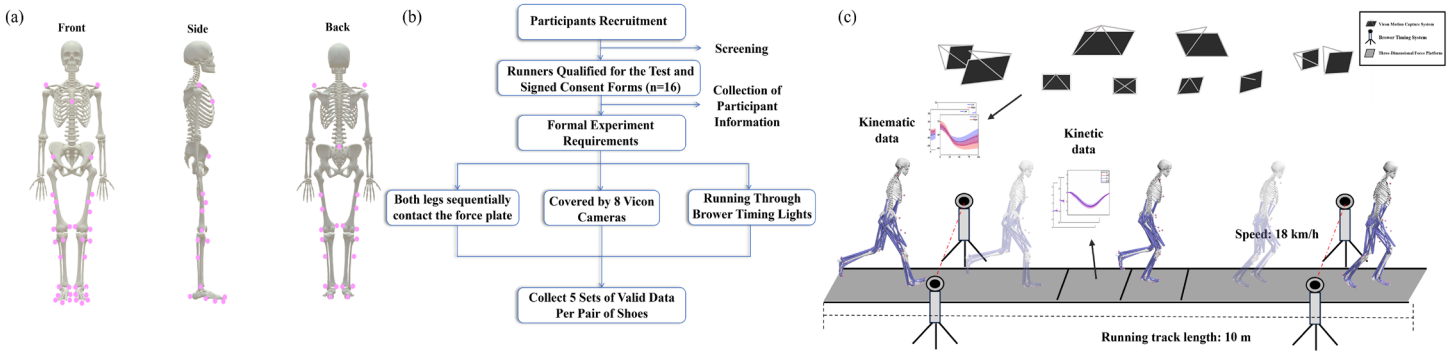

Figure 2. (a) Front, side, and back views with reflective markers, (b) Overview of the experimental procedure, (c) Flowchart of kinematic and kinetic data collection during static and running phases

Data processing

Visual 3D 6.0 (C-Motion Inc., USA) was used to build static and dynamic models based on marker positions and participants' anthropometrics. Joint angles were computed via inverse kinematics, and joint moments were derived using inverse dynamics. All moment data were normalised to body weight to reduce inter-individual variability.

Symmetry between the left and right sides was assessed using the symmetry angle (SA) based on discrete data points. This metric is based on the angle formed by the vector connecting the left and right values in a coordinate system:

$$SA = \frac{\left(45^{\circ} - \arctan\left(\frac{X_{left}}{X_{right}}\right)\right)}{90^{\circ}} \times 100\%$$

If

$$\left(45^{\circ} - \arctan\left(\frac{X_{left}}{X_{right}}\right)\right) > 90^{\circ}$$

Then

$$SA = \frac{\left(45^{\circ} - \arctan\left(\frac{X_{left}}{X_{right}}\right) - 180^{\circ}\right)}{90^{\circ}} \times 100\%$$

Joint stiffness is related to injury and performance, and is defined as follows:

$$K_{joint} = \frac{\Delta M}{ROM}$$

Here, joint stiffness (K_{joint}) was calculated as $\Delta M/ROM$. The stance phase was defined from initial heel contact (heel-strike) to toe-off. Within this interval, ΔM was defined as the difference between the maximum and minimum joint moment of the ankle, knee, and hip (peak-to-peak moment during stance), and ROM was defined as the corresponding difference between the maximum and minimum joint angle (peak-to-peak angle during stance).

Statistical analysis

Data normality was assessed using Shapiro–Wilk tests in SPSS 22.0 (IBM, USA). Continuous joint angle data were analysed via one-dimensional statistical parametric mapping (SPM_1d, paired t-tests) in MATLAB R2022a (MathWorks Inc., USA). Statistical significance was set at $\alpha = 0.05$. Two-way ANOVA compared peak joint moments and stiffness between limbs and shoe types, while paired *t*-tests evaluated differences in symmetry angles of joint ROM, moments,

and stiffness. Given the relatively small, well-trained sample and the limited number of pre-specified scalar outcome variables, no additional across-test correction such as Bonferroni or false discovery rate procedures was applied.

Results

Kinematics

According to the SPM_1d analysis under the flat carbon plate condition (Figure 3), significant bilateral differences were found in hip flexion during early stance (0–18%, $p = 0.043$), with greater flexion on the left side, and in hip abduction during mid-to-late stance (22–94%, $p = 0.001$), with smaller values on the left. Knee extension showed asymmetry in early (0–11%, $p = 0.037$) and mid-to-late stance (29–100%, $p = 0.001$), with directional differences between sides in each phase. Ankle dorsiflexion differed significantly across most of the stance (12–87%, $p = 0.001$), with higher values on the right, and external rotation was also greater on the right in late stance (70–95%, $p = 0.029$).

Under the curved carbon plate condition (Figure 4), SPM_1d analysis revealed significant bilateral differences in hip flexion (27–100%, $p = 0.001$), adduction (74–97%, $p = 0.043$), and internal rotation (93–100%, $p = 0.050$), all greater on the right. Knee extension was also higher on the right during mid-to-late stance (35–100%, $p = 0.001$). At the ankle, right-side plantarflexion (74–89%, $p = 0.001$) and external rotation (0–13%, $p = 0.036$) exceeded left-side values.

Kinetics

As shown in Table 1, both shoe type and limb side significantly affected ankle, knee, and hip joint kinetics.

For the ankle, the inversion ($p = 0.001$) and external rotation moments ($p = 0.044$) were consistently greater on the right. Flexion-extension stiffness differed by shoe type ($p = 0.003$), with significant limb differences ($p = 0.001$) and an interaction effect ($p = 0.001$). Specifically, the flat plate condition showed higher stiffness on the left, whereas no bilateral difference was observed under the curved plate condition.

For the knee joint, peak external rotation moments differed significantly by shoe type and limb ($p = 0.001$), with an interaction effect. The flat plate condition showed higher values on the left, while the curved plate showed the opposite. Flexion-extension stiffness also varied by condition ($p = 0.002$), being higher on the left with flat shoes and on the right with curved ones. In the coronal plane, stiffness differed between shoe types ($p = 0.039$), limbs ($p = 0.001$), and their interaction ($p = 0.018$); however, in both conditions, the left knee showed greater stiffness than the right.

For the hip joint, the peak extension moments differed between shoe types ($p = 0.004$), with higher values on the left under the flat condition and on the right under the curved. Flexion-extension stiffness also varied by shoe type ($p = 0.035$), but remained consistently higher on the left across both conditions. Rotational stiffness in the transverse plane differed significantly by shoe type ($p = 0.002$), with a significant interaction effect ($p = 0.018$); it was higher on the left with flat shoes and on the right with curved shoes.

Symmetry

As shown in Table 2, ankle rotational angle symmetry was significantly poorer in the curved plate condition ($p = 0.046$, $ES = -0.452$), with a 2.7% increase in SA. In contrast, SA values for peak eversion and external rotation moments were reduced by 2.94% and 12.27%, respectively ($p = 0.014$, $ES = 0.571$; $p = 0.016$, $ES = 0.556$), indicating improved symmetry. Frontal plane stiffness symmetry was also worse with the curved plate ($p = 0.032$, $ES = -0.491$), as reflected by a 1.65% increase in SA. Figure 5 illustrates these individual and paired differences in angle, moment, and stiffness symmetry across all planes.

As shown in Table 3, the curved plate condition yielded better symmetry in knee flexion-extension angles and peak external rotation moments, with SA reductions of 4.56% ($p = 0.029$, $ES = 0.501$) and 2.94% ($p = 0.003$, $ES = 0.710$), respectively. However, sagittal plane stiffness symmetry worsened ($p = 0.008$, $ES = -0.622$), with a 4.2% SA increase. In contrast, frontal plane stiffness symmetry improved ($p = 0.044$, $ES = 0.457$), with SA reduced by 2.15%. Figure 6 illustrates individual and paired differences across all knee symmetry metrics.

As shown in Table 4, no significant difference was found in hip flexion-extension angles ($p = 0.202$, $ES = -0.197$), though SA slightly decreased (–1.52%) with the curved plate, suggesting improved symmetry. Conversely, hip rotational angle symmetry worsened ($p = 0.028$, $ES = -0.502$), with SA increasing by 2.73%. In contrast, the curved plate improved symmetry in peak flexion-extension moments ($p = 0.037$, $ES = 0.475$) and rotational stiffness ($p = 0.033$, $ES = 0.485$), with SA reductions of 4.53% and 3.76%, respectively. Figure 7 illustrates individual and paired variations across all hip symmetry metrics.

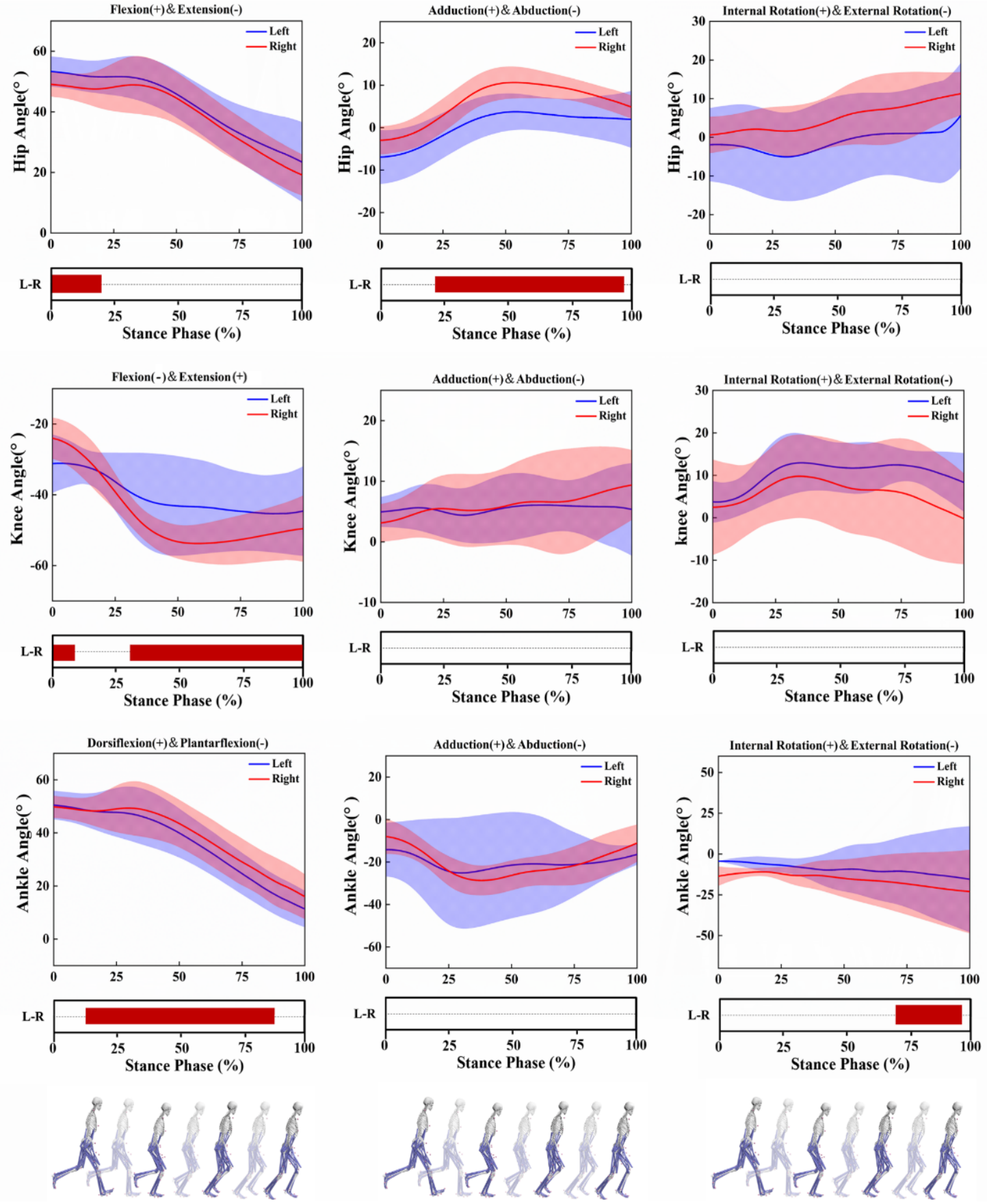

left – left lower limb (non-dominant limb), right – right lower limb (dominant limb)

Figure 3. SPM_1d analysis of joint angle variations during the stance phase in the flat carbon plate shoe condition

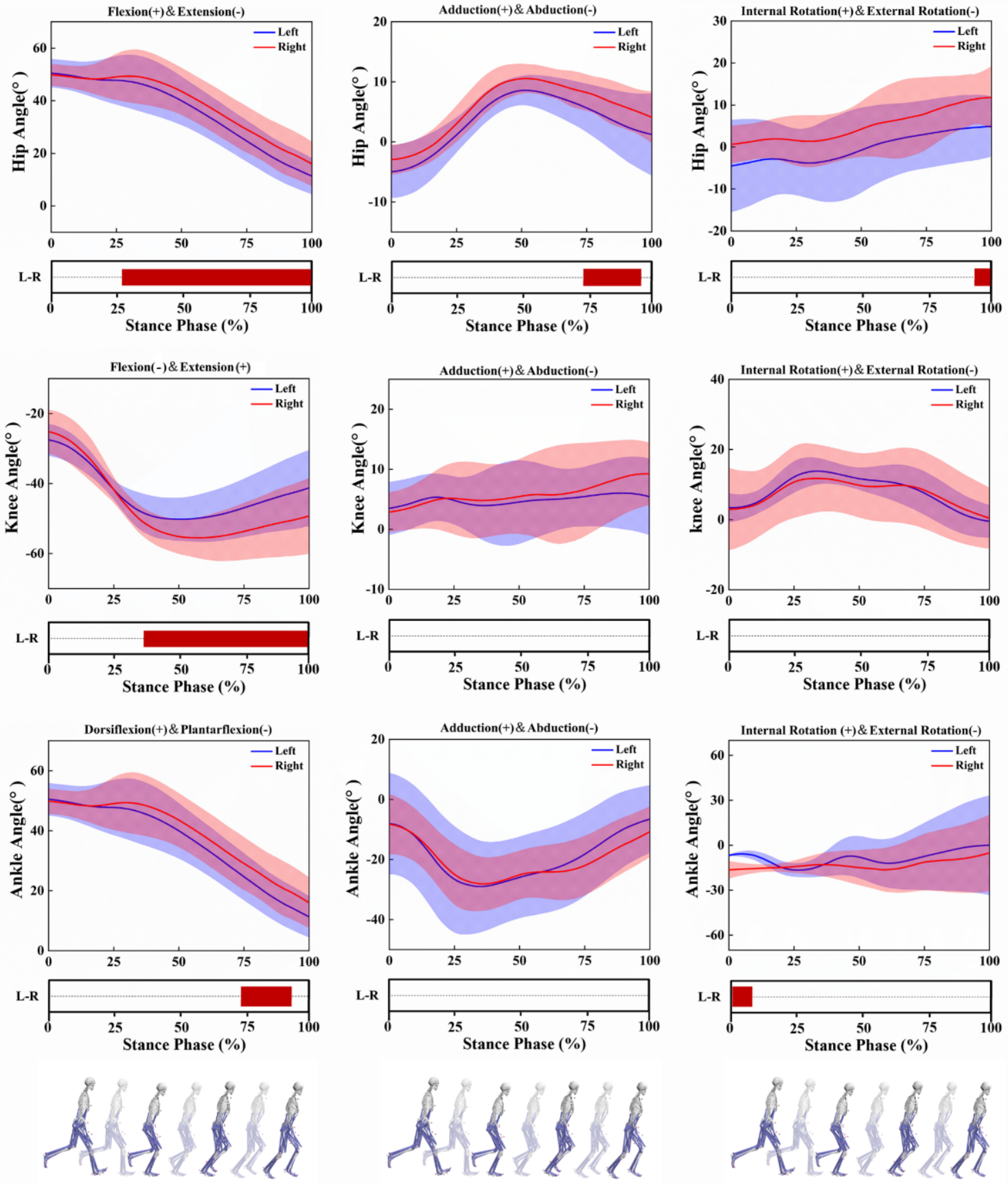

left – left lower limb (non-dominant limb), right – right lower limb (dominant limb)

Figure 4. SPM_1d analysis of joint angle variations during the stance phase in the curved carbon plate shoe condition

Table 1. Comparison of bilateral ankle, knee, and hip joint moments and stiffness between the two carbon plate shoe types

Variables	Flat (mean ± *SD*)		Curved (mean ± *SD*)		Sig.		
	left	right	left	right	S	L	S*L
Ankle joint moment (Nm/kg)							
sagittal	–3.80 ± 1.33	–2.90 ± 0.64	–2.98 ± 0.59	–3.23 ± 0.67	0.158	0.060	0.137
frontal	0.85 ± 0.59	1.38 ± 0.64	1.09 ± 0.65	1.38 ± 0.50	0.322	**0.001***	0.276
horizontal	–0.14 ± 0.04	–0.25 ± 0.16	–0.18 ± 0.04	–0.29 ± 0.19	0.297	**0.044***	0.205
Ankle joint stiffness (Nm/deg)							
sagittal	9.75 ± 3.44	6.12 ± 2.72	6.26 ± 1.21	6.70 ± 1.31	**0.003***	**0.001***	0.001*
frontal	3.73 ± 0.85	4.02 ± 1.82	3.84 ± 1.57	4.20 ± 1.60	0.612	0.192	**0.037***
horizontal	0.82 ± 0.17	0.96 ± 0.67	0.78 ± 0.05	0.83 ± 0.42	0.397	0.129	0.314
Knee joint moment (Nm/kg)							
sagittal	1.89 ± 1.46	2.25 ± 1.27	2.36 ± 0.89	2.52 ± 0.49	0.096	0.242	0.652
frontal	–1.13 ± 0.59	–0.79 ± 0.36	–0.89 ± 0.30	–0.99 ± 0.36	**0.001***	**0.001***	**0.001***
horizontal	–0.23 ± 0.46	–0.27 ± 0.17	–0.21 ± 0.13	–0.17 ± 0.14	0.271	**0.021***	**0.016***
Knee joint stiffness (Nm/deg)							
sagittal	8.45 ± 5.37	6.22 ± 2.94	6.32 ± 2.36	7.30 ± 1.40	**0.006***	**0.002***	0.072
frontal	24.43 ± 3.27	19.80 ± 8.58	22.86 ± 6.91	17.27 ± 5.96	**0.039***	**0.001***	0.018*
horizontal	1.24 ± 0.73	1.41 ± 0.85	0.93 ± 0.30	1.50 ± 0.54	0.217	0.929	0.328
Hip joint moment (Nm/kg)							
sagittal	–5.76 ± 1.23	–3.49 ± 1.54	–3.34 ± 1.14	–4.02 ± 1.69	**0.004***	0.100	0.052
frontal	–2.01 ± 0.46	–1.74 ± 0.71	–1.67 ± 0.40	–2.01 ± 0.71	0.761	0.739	**0.011***
horizontal	0.54 ± 0.22	0.41 ± 0.23	0.45 ± 0.16	0.50 ± 0.21	0.096	0.062	0.214
Hip joint stiffness (Nm/deg)							
sagittal	6.12 ± 2.39	5.38 ± 2.33	5.80 ± 1.45	4.89 ± 2.20	**0.035***	0.140	0.067
frontal	10.68 ± 2.37	8.38 ± 3.42	9.23 ± 2.22	10.24 ± 3.18	0.718	0.256	0.479
horizontal	4.98 ± 1.08	2.89 ± 1.45	2.32 ± 0.88	4.14 ± 1.72	**0.002***	0.101	0.018*

left – left lower limb (non-dominant), right – right lower limb (dominant), sagittal – flexion-extension, frontal – abduction-adduction, horizontal – rotation, S – shoe types, L – limbs, S*L – shoe types and limbs interaction
* indicates significant differences ($p < 0.05$)
Bold values indicate statistical significance.

Table 2. Comparison of ankle joint angle, moment, and stiffness SA results between the two carbon plate shoe types

Ankle	Symmetry angle (%)			
	flat (mean ± *SD*)	curved (mean ± *SD*)	Sig.	*ES* (Cohen's *d*)
Joint angle				
sagittal	3.73 ± 2.41	4.28 ± 2.26	0.212	–0.274
frontal	8.64 ± 6.23	6.93 ± 4.13	0.331	0.212
horizontal	22.67 ± 4.51	25.37 ± 6.76	**0.046***	–0.452
Joint moment				
sagittal	13.55 ± 11.43	11.13 ± 5.98	0.180	0.296
frontal	5.61 ± 4.18	2.67 ± 1.48	**0.014***	0.571
horizontal	25.32 ± 11.25	13.05 ± 7.73	**0.016***	0.556
Joint stiffness				
sagittal	11.36 ± 6.90	8.66 ± 4.89	0.057	0.430
frontal	2.71 ± 1.23	4.36 ± 3.69	**0.032***	–0.491
horizontal	20.13 ± 10.09	17.46 ± 8.43	0.082	0.389

sagittal – flexion-extension, frontal – abduction-adduction, horizontal – rotation
* indicates significant differences ($p < 0.05$)
Bold values indicate statistical significance

Table 3. Comparison of knee joint angle, moment, and stiffness SA results between the two carbon plate shoe types

Knee	Symmetry angle (%)			
	flat (mean ± *SD*)	curved (mean ± *SD*)	Sig.	*ES* (Cohen's *d*)
Joint angle				
sagittal	10.77 ± 7.40	6.21 ± 5.19	**0.029***	0.501
frontal	9.83 ± 5.47	10.77 ± 7.40	0.580	–0.120
horizontal	11.32 ± 9.25	13.05 ± 6.43	0.092	–0.377
Joint moment				
sagittal	26.38 ± 19.86	24.13 ± 11.05	0.341	–0.208
frontal	9.42 ± 5.12	5.77 ± 4.32	**0.003***	0.710
horizontal	18.11 ± 5.22	20.65 ± 4.98	0.063	–0.419
Joint stiffness				
sagittal	20.62 ± 12.42	24.82 ± 8.64	**0.008***	–0.622
frontal	7.73 ± 6.44	5.58 ± 3.94	**0.044***	0.457
horizontal	6.86 ± 3.22	7.08 ± 4.88	0.861	–0.038

sagittal – flexion-extension, frontal – abduction-adduction, horizontal – rotation
* indicates significant differences ($p < 0.05$
Bold values indicate statistical significance

Table 4. Comparison of hip joint angle, moment, and stiffness SA results between the two carbon plate shoe types

Hip	Symmetry angle (%)			
	flat (mean ± *SD*)	curved (mean ± *SD*)	Sig.	*ES* (Cohen's *d*
Joint angle				
sagittal	10.39 ± 4.77	8.87 ± 3.73	0.202	–0.197
frontal	7.86 ± 5.51	6.82 ± 4.74	0.331	–0.212
horizontal	11.32 ± 9.25	14.05 ± 6.43	**0.028***	–0.502
Joint moment				
sagittal	9.68 ± 4.12	5.15 ± 4.32	**0.037***	0.475
frontal	7.03 ± 3.79	5.89 ± 4.97	0.418	0.176
horizontal	11.07 ± 6.98	9.86 ± 3.79	0.391	0.187
Joint stiffness				
sagittal	20.19 ± 15.61	18.32 ± 10.42	0.538	0.133
frontal	10.53 ± 8.35	8.66 ± 4.57	0.063	0.419
horizontal	12.13 ± 8.73	8.37 ± 7.11	**0.033***	0.485

sagittal – flexion-extension, frontal – abduction-adduction, horizontal – rotation
* indicates significant differences ($p < 0.05$
Bold values indicate statistical significance

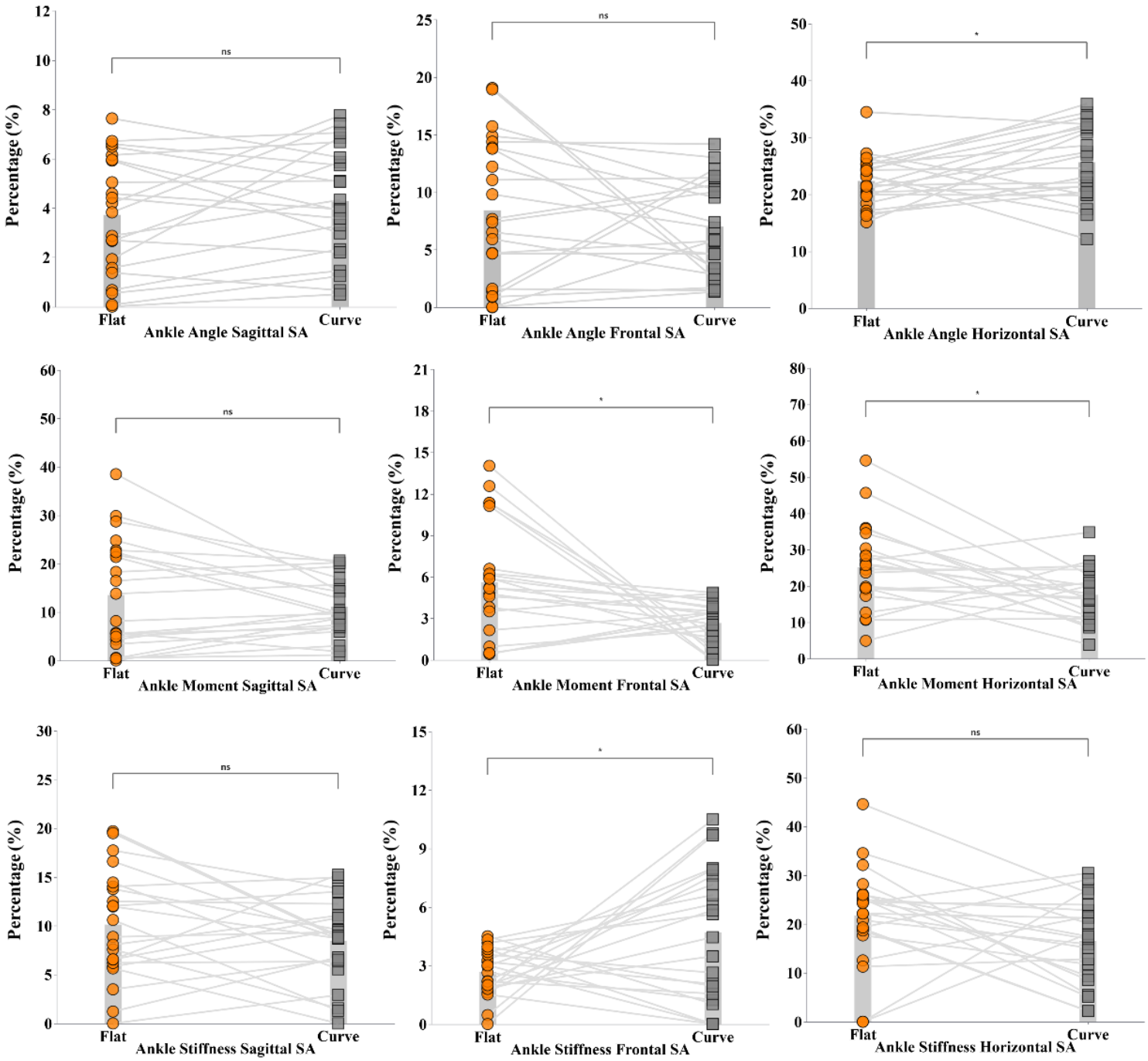

Figure 5. Paired dot plots comparing the SA of ankle joint angle, moment, and stiffness between the two carbon plate shoe types

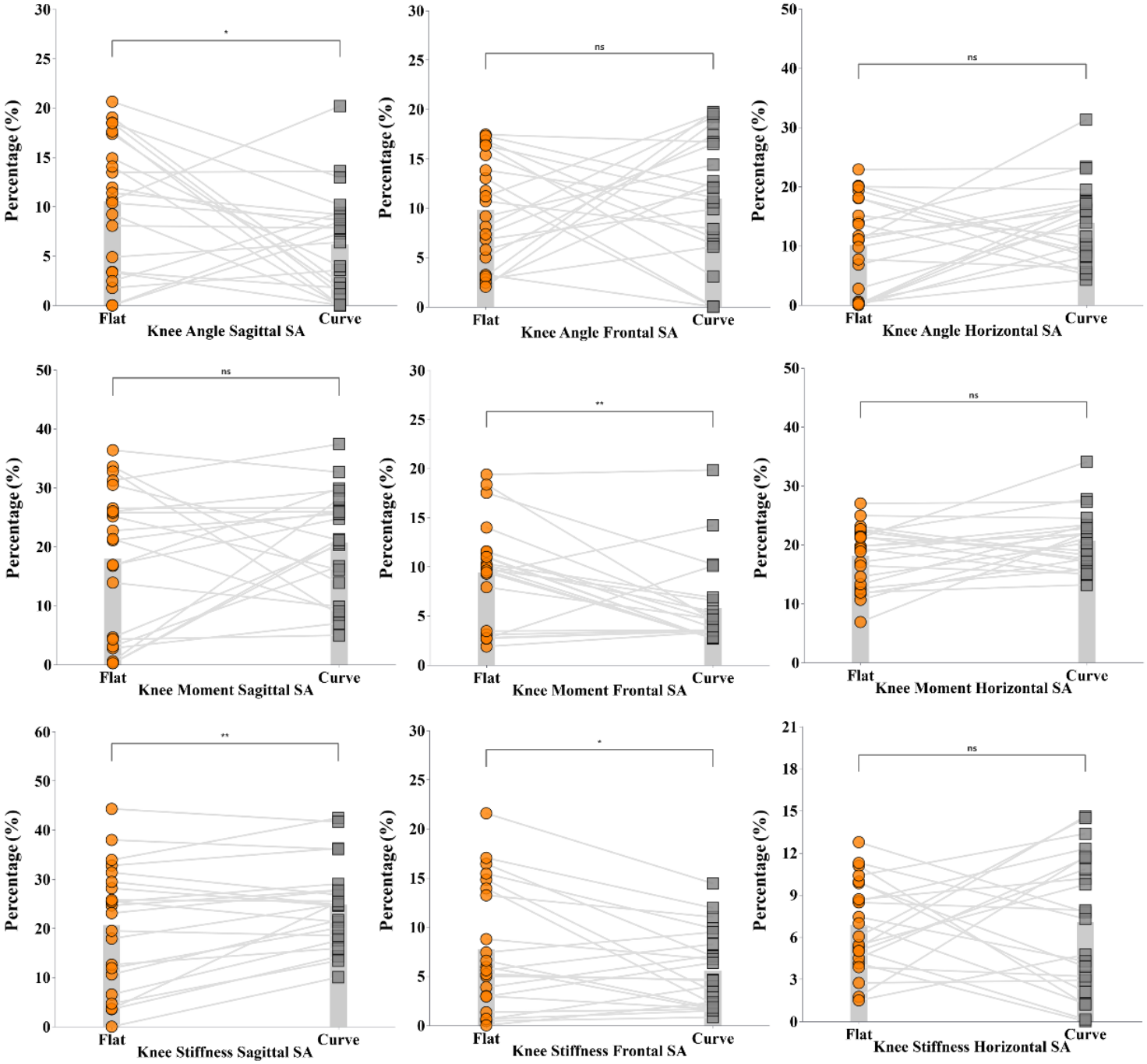

Figure 6. Paired dot plots comparing the SA of knee joint angle, moment, and stiffness between the two carbon plate shoe types

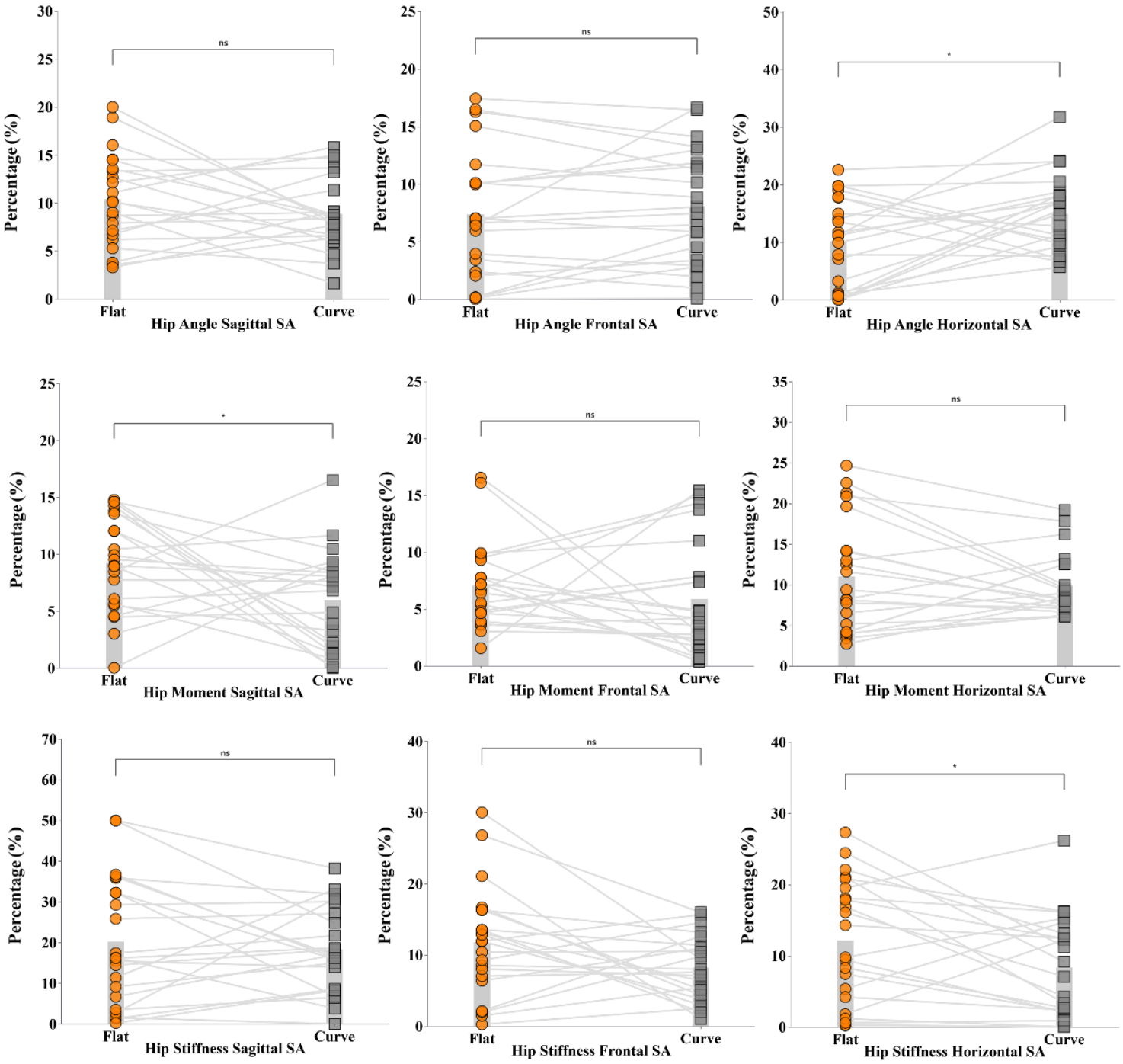

Figure 7. Paired dot plots comparing the SA of hip joint angle, moment, and stiffness between the two carbon plate shoe types

Discussion

This study examined how flat and curved carbon plate shoe designs affect lower limb joint symmetry in well-trained marathon runners. The results showed that plate geometry significantly influenced joint kinematics and kinetics, particularly symmetry. The curved plate improved symmetry in select ankle and knee kinetic variables, despite minor asymmetries in kinematics, highlighting its role in modulating lower limb symmetry during running.

The carbon plate geometry affected hip joint symmetry in a phase-specific manner. The flat plate induced greater left-side hip flexion during early stance, while the curved plate increased right-side hip flexion, adduction, and internal rotation during mid-to-late stance. These differences likely reflect variations in load distribution: the flat design may heighten initial impact on the left side, requiring greater flexion for stabilisation, whereas the curved design facilitates smoother foot rollover [1] but may elevate asymmetry in hip motion, which may theoretically increase the risk of hip joint overload and related overuse problems [20].

Knee joint symmetry differed between the two shoe types. The flat plate showed reduced right knee extension early in the stance and greater extension later, while the curved plate consistently exhibited larger right knee extension angles throughout. These phase shifts may cause uneven joint loading, increasing the risk of instability and tibial stress injuries [21]. Kinetically, the curved plate improved symmetry in external rotation moments and coronal stiffness, suggesting more balanced load distribution and a more favourable profile of overuse-related injury risk factors. From a lower limb kinetic chain perspective, such knee-level changes are unlikely to occur in isolation. Improved frontal plane knee symmetry may partly reflect altered hip neuromuscular control and ankle and foot rollover mechanics, and may influence how the hip and ankle are loaded during stance [22]. Enhancing knee load symmetry is widely considered important for managing biomechanical risk factors underlying chronic injuries, especially in high-load training for well-trained runners [23]. The results thus suggest that the improvements in symmetry are primarily associated with differences in plate geometry, while acknowledging that other midsole and rocker parameters may also have played a role.

Ankle joint kinematics were strongly influenced by carbon plate geometry. The flat plate increased right-side dorsiflexion across much of the stance, possibly due to its straight design limiting forefoot flexion and disrupting efficient force transfer [4]. In contrast, the curved plate enhanced right-side plantarflexion during late stance, likely by better matching the foot's arch and improving rollover mechanics [3]. Kinetically, the curved plate improved symmetry in ankle eversion and external rotation moments by promoting more uniform plantar pressure and balanced moment generation [24]. This may reduce compensatory actions in proximal joints, enhancing overall stability. However, the curved design may limit rotational mobility, increasing stiffness and reducing adaptive capacity during stance [25]. In some cases, it may elevate midfoot loading, reducing the ankle's shock-absorbing function and increasing rotational stiffness during propulsion [26]. These findings highlight a trade-off between support and flexibility with curved plate designs [27].

This study found that the carbon plate shape significantly influenced the stiffness symmetry in the ankle, knee, and hip joints, with notable interaction effects. While the curved plate improved knee stiffness symmetry in the coronal plane, it reduced that of the ankle, highlighting that biomechanical responses extend beyond individual joints and reflect inter-joint interactions across the kinetic chain [28]. Such asymmetries may trigger compensatory muscle activation or contralateral overloading, potentially increasing the risk of tendinopathy or joint degeneration over time [10, 29]. Future studies should incorporate both EMG and in-shoe plantar pressure measurements to assess how carbon plate geometry modulates stiffness symmetry, neuromuscular patterns, and local plantar loading, thereby aiding the development of designs that enhance performance and address biomechanical risk factors for injury [30, 31].

Carbon plate geometry affects not only individual joint mechanics but also overall lower limb coordination via the kinetic chain. This study revealed inconsistent joint responses to plate shape, suggesting potential disruption in movement coordination and reduced efficiency over time. Prior studies have linked poor coordination with increased energy cost and higher risks of chronic injuries such as stress fractures, Achilles tendinopathy, and iliotibial band syndrome [32, 33]. For well-trained marathoners, even small asymmetries can compound with long-term training, elevating injury risk. In this context, the SA changes observed in our study should be viewed as small but systematic deviations from perfect symmetry that may help identify runners who warrant closer monitoring rather than as indicators of overt pathology. Longitudinal studies are therefore needed to evaluate the sustained effects of carbon plate design on coordination and on biome-

chanical indicators related to injury risk, guiding shoe design that balances performance with safety.

Despite systematically investigating the impact of carbon plate geometry on lower limb symmetry and kinetics in well-trained marathon runners, this study has limitations. First, the fixed running speed may not reflect effects across varying intensities, limiting the generalisability of the results. Second, the exclusive inclusion of well-trained, healthy male runners employing a rear-foot strike running technique restricts the applicability to broader populations, and the present findings may not be generalisable to female runners. Third, lab-based testing, though precise, lacks the ecological validity of real-world running environments. Fourth, plantar pressure data were not collected, which precludes a direct link between joint-level asymmetry, local plantar loading patterns, and potential stress fracture risk. Future studies should integrate in-shoe plantar pressure measurements and include more diverse participant samples in outdoor running conditions to better characterise how carbon plate geometry affects joint mechanics and local tissue loading, thereby improving the practical relevance of design recommendations for performance and injury prevention [34]. In addition, applying artificial intelligence and machine learning to these datasets may help identify subtle movement patterns and improve data-driven injury risk prediction in carbon plate footwear research [35, 36].

Conclusions

This study demonstrated that carbon plate geometry meaningfully modulates lower limb biomechanical symmetry in well-trained marathon runners. Curved plates were associated with improved symmetry in ankle inversion–eversion and internal–external rotation moments, knee adduction–abduction moments and stiffness, and hip rotational stiffness, which may promote more balanced lower-limb load distribution and help mitigate injury risk. In contrast, flat plates yielded more symmetrical hip rotational angles and knee flexion–extension stiffness, suggesting a potential advantage for maintaining coordinated lower-limb movement. Taken together, these plane-specific effects highlight plate shape as a functional design parameter and offer practical guidance for optimising carbon-plated shoe design and using lower-limb symmetry profiles in athlete screening and monitoring.

Acknowledgements

The authors would like to thank all the subjects who selflessly participated in the study.

Ethical approval

The research related to human use complied with all the relevant national regulations and institutional policies, followed the tenets of the Declaration of Helsinki, and was approved by the Ethics Committee of Ningbo University (approval No.: TY2025051).

Informed consent

Informed consent was obtained from all individuals included in this study.

Conflicts of interest

The authors declare no conflicts of interest.

Disclosure statement

No author has any financial interest or received any financial benefit from this research.

Funding

This research received funding from the National Key R&D Program of China (2024YFC3607305), Zhejiang Province Science Fund for Distinguished Young Scholars (LR22A020002), Zhejiang Provincial Key Project of Education Science Planning (2025SB084), Zhejiang Engineering Research Center for New Technologies and Applications of Helium-Free Magnetic Resonance Imaging Open Fund Project 2024 (2024GCPY02, 2024GCPY06), Ningbo Key Research and Development Program (2022Z196), Zhejiang Rehabilitation Medical Association Scientific Research Special Fund (ZKKY2023001), Research Academy of Medicine Combining Sports, Ningbo (No.2023001), Ningbo Clinical Research Center for Orthopedics and Exercise Rehabilitation (No.2024L004), Ningbo Natural Science Foundation (2022J065), and the K. C. Wong Magna Fund at Ningbo University.

References

[1] Song Y, Cen X, Chen H, Sun D, Munivrana G, Bálint K, Bíró I, Gu Y. The influence of running shoe with different carbon-fiber plate designs on internal foot mechanics: a pilot computational analysis. J Biomech. 2023;153:111597; doi: 10.1016/j.jbiomech.2023.111597.

[2] Chen H, Shao E, Sun D, Xuan R, Baker JS, Gu Y. Effects of footwear with different longitudinal bending stiffness on biomechanical characteristics and muscular mechanics of lower limbs in adolescent runners. Front Physiol. 2022;13:907016; doi: 10.3389/fphys.2022.907016.

[3] Song Y, Cen X, Sun D, Bálint K, Wang Y, Chen H, Gao S, Bíró I, Zhang M, Gu Y. Curved carbon-

plated shoe may further reduce forefoot loads compared to flat plate during running. Sci Rep. 2024;14(1):13215; doi: 10.1038/s41598-024-64177-3.

[4] Xu Y, Zhu C, Fang Y, Lu Z, Song Y, Hu C, Sun D, Gu Y. The effects of different carbon-fiber plate shapes in shoes on lower limb biomechanics following running-induced fatigue. Front Bioeng Biotech. 2025;13:1539976; doi: 10.3389/fbioe.2025.1539976.

[5] Gao Z, Fekete G, Baker JS, Liang M, Xuan R, Gu Y. Effects of running fatigue on lower extremity symmetry among amateur runners: from a biomechanical perspective. Front Physiol. 2022;13:899818; doi: 10.3389/fphys.2022.899818.

[6] Gao S, Song Y, Sun D, Cen X, Wang M, Lu Z, Gu Y. Impact of Becker muscular dystrophy on gait patterns: insights from biomechanical analysis. Gait Posture. 2025;121:160–165; doi: 10.1016/j.gaitpost.2025.05.008.

[7] Cai J, Liu Q, Chen H, Xu Y, Dong S, Rong M, Gu Y. A biomechanical study of lower limb distal joint asymmetry during running using bionic shoe. Molecul Cell Biomech. 2025;22(4):323; doi: 10.62617/mcb323.

[8] Larsen P, Laessoe U, Rasmussen S, Graven-Nielsen T, Eriksen CB, Elsoe R. Asymmetry in gait pattern following tibial shaft fractures–a prospective one-year follow-up study of 49 patients. Gait Posture. 2017;51:47–51; doi: 10.1016/j.gaitpost.2016.09.027.

[9] Guan Y, Bredin SS, Taunton J, Jiang Q, Wu N, Warburton DE. Association between inter-limb asymmetries in lower-limb functional performance and sport injury: a systematic review of prospective cohort studies. J Clin Med. 2022;11(2):360; doi: 10.3390/jcm11020360.

[10] Helme M, Tee J, Emmonds S, Low C. Does lower-limb asymmetry increase injury risk in sport? A systematic review. Phys Ther Sport. 2021;49:204–13; doi: 10.1016/j.ptsp.2021.03.001.

[11] Seymore KD, Corrigan P, Sigurðsson HB, Pohlig RT, Silbernagel KG. Asymmetric running is associated with pain during outdoor running in individuals with Achilles tendinopathy in the return-to-sport phase. Phys Ther Sport. 2024;67:25–30; doi: 10.1016/j.ptsp.2024.02.006.

[12] Beck ON, Azua EN, Grabowski AM. Step time asymmetry increases metabolic energy expenditure during running. Eur J Appl Physiol. 2018;118(10):2147–54; doi: 10.1007/s00421-018-3939-3.

[13] Luftglass AR, Peebles AT, Miller TK, Queen RM. The impact of standardized footwear on load and load symmetry. Clin Biomech. 2021;88:105421; doi: 10.1016/j.clinbiomech.2021.105421.

[14] Jandová S, Sparks M, Oleśniewicz P, Charousek J, Chrástková M, Markiewicz J. Changes in the foot strike pattern and pressure distribution when running in minimalist and traditional sport shoes. Med Sport. 2018;71(2):257–67; doi: 10.23736/S0025-7826.18.03029-6.

[15] Jandova S, Volf P, Vaverka F. The influence of minimalist and conventional sports shoes and lower limbs dominance on running gait. Acta of Bioeng Biomech. 2018;20(3):3–9; doi: 10.5277/ABB-01120-2018-02.

[16] Zhu C, Song Y, Xu Y, Zhu A, Baker JS, Liu W, Gu Y. Toe box shape of running shoes affects in-shoe foot displacement and deformation: a randomized crossover study. Bioeng. 2024;11(5):457; doi: 10.3390/bioengineering11050457.

[17] Dhahbi W: Editioral: Advancing biomechanics: enhancing sports performance, mitigating injury risks, and optimizing athlete rehabilitation. Front Sports Act Living. 2025;7:1556024; doi: 10.3389/fspor.2025.1556024.

[18] Puig-Diví A, Escalona-Marfil C, Padullés-Riu JM, Busquets A, Padullés-Chando X, Marcos-Ruiz D. Validity and reliability of the Kinovea program in obtaining angles and distances using coordinates in 4 perspectives. PLOS ONE. 2019;14(6):e0216448; doi: 10.1371/journal.pone.0216448.

[19] Cen X, Yu P, Song Y, Sun D, Liang M, Bíró I, Gu Y. Influence of medial longitudinal arch flexibility on lower limb joint coupling coordination and gait impulse. Gait Posture, 2024;114:208–14; doi: 10.1016/j.gaitpost.2024.10.002.

[20] Foch E, Brindle RA, Pohl MB. Lower extremity kinematics during running and hip abductor strength in iliotibial band syndrome: a systematic review and meta-analysis. Gait Posture. 2023;101:73–81; doi: 10.1016/j.gaitpost.2023.02.001.

[21] Dong X, Li C, Liu J, Huang P, Jiang G, Zhang M, Zhang W, Zhang X. The effect of running on knee joint cartilage: a systematic review and meta-analysis. Phy Ther Sport. 2021;47:147–55; doi: 10.1016/j.ptsp.2020.11.030.

[22] Dhahbi W, Materne O, Chamari K. Rethinking knee injury prevention strategies: joint-by-joint training approach paradigm versus traditional focused knee strengthening. Biol Sport. 2025;42(4):59–65; doi: 10.5114/biolsport.2025.148544.

[23] Gao Z, Mei Q, Fekete G, Baker JS, Gu Y. The effect of prolonged running on the symmetry of biomechanical variables of the lower limb joints. Symmetry. 2020;12(5):720; doi: 10.3390/sym12050720.
[24] Miyazaki T, Aimi T, Yamada Y, Nakamura Y. Curved carbon plates inside running shoes modified foot and shank angular velocity improving mechanical efficiency at the ankle joint. J Biomech. 2024;172:112224; doi: 10.1016/j.jbiomech.2024.112224.
[25] Hébert-Losier K, Pamment M. Advancements in running shoe technology and their effects on running economy and performance – a current concepts overview. Sports Biomech. 2023;22(3):335–50; doi: 10.1080/14763141.2022.2110512.
[26] Stefanyshyn DJ, Wannop JW. The influence of forefoot bending stiffness of footwear on athletic injury and performance. Footwear Sci. 2016;8(2):51–63; doi: 10.1080/19424280.2016.1144652.
[27] Cigoja S, Firminger CR, Asmussen MJ, Fletcher JR, Edwards WB, Nigg BM. Does increased midsole bending stiffness of sport shoes redistribute lower limb joint work during running? J Sci Med Sport. 2019;22(11):1272–77; doi: 10.1016/j.jsams.2019.06.015.
[28] Furlong L-A, Egginton NL. Kinetic asymmetry during running at preferred and nonpreferred speeds. Med Sci Sports Exerc, 2018;50(6):1241–48; doi: 10.1249/MSS.0000000000001560.
[29] Koźlenia D, Struzik A, Domaradzki J. Force, power, and morphology asymmetries as injury risk factors in physically active men and women. Symmetry. 2022;14(4):787; doi:10.3390/sym14040787.
[30] Cigoja S, Fletcher JR, Esposito M, Stefanyshyn DJ, Nigg BM. Increasing the midsole bending stiffness of shoes alters gastrocnemius medialis muscle function during running. Sci Rep. 2021;11(1):749; doi: 10.1038/s41598-020-80791-3.
[31] Tajik R, Dhahbi W, Fadaei H, Mimar R. Muscle synergy analysis during badminton forehand overhead smash: integrating electromyography and musculoskeletal modeling. Front Sports Act Living. 2025;7:1596670; doi: 10.3389/fspor.2025.1596670.
[32] Wren TA, Mueske NM, Brophy CH, Pace JL, Katzel MJ, Edison BR, Vandenberg,CD, Zaslow TL. Hop distance symmetry does not indicate normal landing biomechanics in adolescent athletes with recent anterior cruciate ligament reconstruction. J Orthop Sports Phys Ther. 2018;48(8):622–9; doi: 10.2519/jospt.2018.7817.
[33] Wang J, Qin Z, Zhang Q, Wang J. Lower limb dynamic balance, strength, explosive power, agility, and injuries in volleyball players. J Orthop Surg Res. 2025;20(1):211; doi: 10.1186/s13018-025-05566-w.
[34] Tessutti V, Diniz AA, Signorini L, Soares HB, Vidotto MC, Yi LC. Sonification of plantar pressure in runners with and without pain after running practice. Hum Mov. 2024;25(1):123–30; doi: 10.5114/hm.2024.136931.
[35] Souaifi M, Dhahbi W, Jebabli N, Ceylan Hİ, Boujabli M, Muntean RI, Dergaa I. Artificial intelligence in sports biomechanics: a scoping review on wearable technology, motion analysis, and injury prevention. Bioengineering. 2025;12(8):887; doi: 10.3390/bioengineering12080887.
[36] Song Y, Cen X, Wang M, Gao Z, Tan Q, Sun D, Gu Y, Wang Y, Zhang M. A systematic review of finite element analysis in running footwear biomechanics: insights for running-related musculoskeletal injuries. J Sports Sci Med. 2025;24(2):370–87; doi: 10.52082/jssm.2025.370.